Journal of Materials Chemistry C

Nonlinear optical enhancement caused by a higher order multipole mode of metallic triangles

Journal:	*Journal of Materials Chemistry C*
Manuscript ID:	TC-ART-10-2014-002427.R1
Article Type:	Paper
Date Submitted by the Author:	03-Dec-2014
Complete List of Authors:	Kolaric, Branko; UNIVERSITE MONS, INFLUX lab van der Veen, Monique; Delft University of Technology, Catalysis Engineering Verbiest, Thierry; KU Leuven, Chemistry Maes, Bjorn; UMONS, Micro Photonics Vanbeel, Maarten; KU Leuven, Chemistry Rosolen, Gilles; UMONS, Micro Photonics

Nonlinear optical enhancement caused by a higher order multipole mode of metallic triangles

Monique van der Veen[1,2,*] Gilles Rosolen[3], Thierry Verbiest[1], Maarten K. Vanbel[1], Bjorn Maes[3], and Branko Kolaric[4†]

[1]*Deparment of Chemistry, University of Leuven, Celestijnenlaan 200D, B-3001 Heverlee, Belgium* [2]*Catalysis Engineering, Applied Sciences, Delft University of Technology, Julianalaan 136, 2628 BL, Delft, the Netherlands* [3]*Micro- and Nanophotonic Materials Group, Faculty of Science, University of Mons, 20 Place du Parc, B-7000 Mons, Belgium* [4]*Laboratoire Interfaces and Fluides Complexes, Centre d'Innovation et de Recherche en Materiaux Polymeres, University of Mons, 20 Place du Parc, B-7000 Mons, Belgium*

(Dated: December 3, 2014)

Abstract

We describe a nonlinear optical study of gold triangles that exploits a higher order plasmonic resonance. A comprehensive nonlinear optical characterisation was performed both by second harmonic generation (SHG) and two photon fluorescence spectroscopy (2PF). We demonstrate and explain the enhancement of the coherent and incoherent nonlinear optical emission by a higher order multipolar mode of the plasmonic structure. The peculiarities of the mode shape and its influence on intensity and polarisation of the nonlinear signal are experimentally and numerically confirmed.

*Electronic address: M.A.vanderVeen@tudelft.nl

†Electronic address: branko.kolaric@umons.ac.be

I. INTRODUCTION

Localized surface plasmon polaritons (LSPPs) and surface plasmon polaritons (SPPs) are electromagnetic excitations coupled to the electron charge density waves localized on metallic nanostructures and metal-dielectric interfaces, respectively. These modes allow for confinement of light at the nanoscale level (10-100 nm), far below conventional optics [1],[2]. Additionally, in modern nano-optics plasmonic resonances become important as they offer a unique and distinctive way for controlling light emission by coupling radiation of a nanoprobe (molecule, quantum dot etc.) with the environment [3],[4],[5].

Recently, nonlinear optical effects attract special attention as strong electromagnetic fields in the vicinity of metallic structures generate a significant enhancement of the nonlinear processes, which depend super-linearly on the local fields [2]. Moreover, the ability to convert low-energy quanta into a quantum of higher energy is crucial for a variety of applications, including bioimaging, drug delivery, photovoltaics and solar cell technology [2]. However, the majority of reported optical studies considering metallic particles and their arrays have been performed only in the linear optical regime using transmission, reflection and fluorescence spectroscopy [6],[7],[8]. Up to now, a number of metallic nanostructures of diverse architectures have been studied by nonlinear optical techniques [2],[10],[9], .

Structures such as gold metallic triangles (i.e. curved nanotriangles and nanoprisms) attract interest because of their antenna effect. The latter effect creates a huge enhancement of electromagnetic fields in the vicinity of tips [10],[14],[15][16]. Furthermore, recent investigations of gold triangles point out the mutual importance of the resonance position and tip-to-tip orientation for their optical response [19],[13],[14]. Recently, plasmonic circuitry at the micrometer scale made from metallic nanotriangles and nanoprisms was demonstrated with potential applications in telecommunication technology [17],[18]. Likewise, it has been indicated [2],[10] that nanotriangles are promising candidates for various applications such as photonic circuits, super-resolution imaging, enhanced fluorescence and Raman detection.

Despite a tremendous number of publications, the higher order modes are seldom examined and the dipolar mode is preferentially used for enhancement of an optical signal [2],[20],[21]. However, for various potential applications (especially for sensing using linear or nonlinear emission) the dipole mode is probably a less attractive resonance, because the strong electric field generated by incoming light (matching between dipole mode and

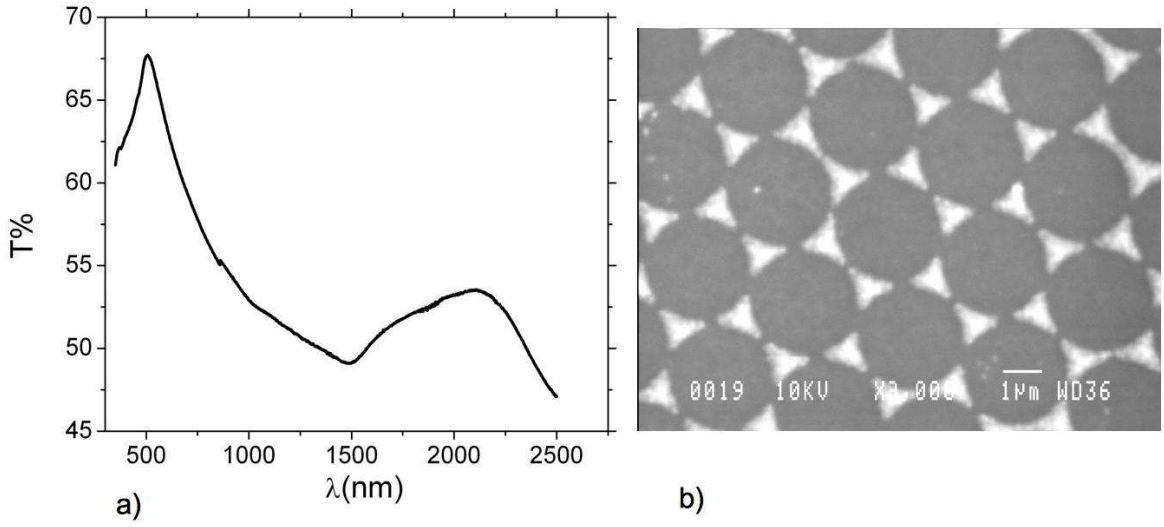

Figure 1: (a) Measured transmission spectrum of the gold triangle array. (b) SEM image of the array, with the 1 μm scale bar.

fundamental wavelength) can trigger nanopatterning processes [20],[22],[23].

In this article a comprehensive nonlinear optical study of gold metallic triangles is described using two different nonlinear optical techniques, coherent second harmonic generation (SHG) and incoherent two-photon fluorescence (2PF) spectroscopy. With these two techniques we are able to reveal the effect of the higher order and less studied mode on the enhancement of the coherent and incoherent nonlinear emission.

II. RESULTS AND DISCUSSION

The triangular gold nanoparticles in this study are made by nanosphere lithography utilising the drop coating method of Micheletto [11],[12] as used by Kolaric and Morarescu [13]. The technique employs nanospheres dispersed in solution to create a close-packed monolayer with hexagonal symmetry, which is employed as a mask in a subsequent step, where gold is deposited (40 nm) through the nanospheres to fill the void spaces in the layer lattice. Regular arrays of triangular gold nanoparticles are fabricated in a last step, when the nanosphere mask is removed. The corresponding metallic triangles (Figure 1b) were chosen due to the relatively good matching between the higher order plasmonic resonance and the wavelength of the fundamental.

A top-view scanning electron microscope (SEM) image (Figure 1b) shows the size and the shape of the metallic triangles (side $\sim$ 900 nm) as well as the exceptionally good ordering of triangles within the array. The optical properties of metallic particles are influenced by the particle size and orientation. Therefore, by increasing the size a higher order plasmon mode appears in the extinction spectrum (Figure 1a) [13],[23],[25],[26]. Additionally, the higher order plasmon bandwidth can become broader as a result of more radiative damping. In our case, the transmission spectrum of the gold metallic triangles (Figure 1a) consists of two main dips (and thus extinction maxima): a small dip (between 500 nm and 1800 nm, with a minimum around 1500 nm), originating from a higher order mode of the triangles, and a main dip (above 2500 nm) in the near infrared domain, related to the dipole mode [13]. The dipolar minimum is beyond our experimental data, however these dipole and higher order modes have also been identified in previous work [13]. In the aricle published by Morarescu et al, dipolar and higher order modes of nanotriangles of different size are fully described and discussed.

The nonlinear optical study of the gold triangles was performed using a wide field nonlinear optical microscope [27],[28]. Figure 2a shows an optical image of the array studied in our experiments, while the nonlinear responses are recorded by imaging 2PF and SHG as a function of polarisation (Figure 2b and 2c, respectively). The wavelength of the fundamental (800 nm) overlaps with the broadband higher order mode resonance of the gold triangle. Furthermore, Figure 2 confirms that the observed enhancement is not related to the presence of a local defect within the array (the yellow line indicates a defect).

Figures 2b and 2c show merged 2PF- and SHG-images, which consist of three combined images with different colour, where each colour corresponds to a different plane of polarisation of the incident light. The depicted incident polarisations are chosen such that they coincide with an orientation of the triangle edges. These images indicate that each triangle tip generates the nonlinear optical light independently: the response of each tip is spatially resolved from the responses of the other two tips of the same triangle, as well as from the tip of the neighbouring triangles. The pattern of the array is clearly visible in the nonlinear response, pointing out that the observed response is directly related to the plasmonic structure itself. The figure shows a defect in the Au-triangle array (see yellow line as guid to the eye) where no SHG and 2PF is generated. In fact the intensity along this defect corresponds to the noise level in the SHG and 2PF images. With regard to the standard deviation of

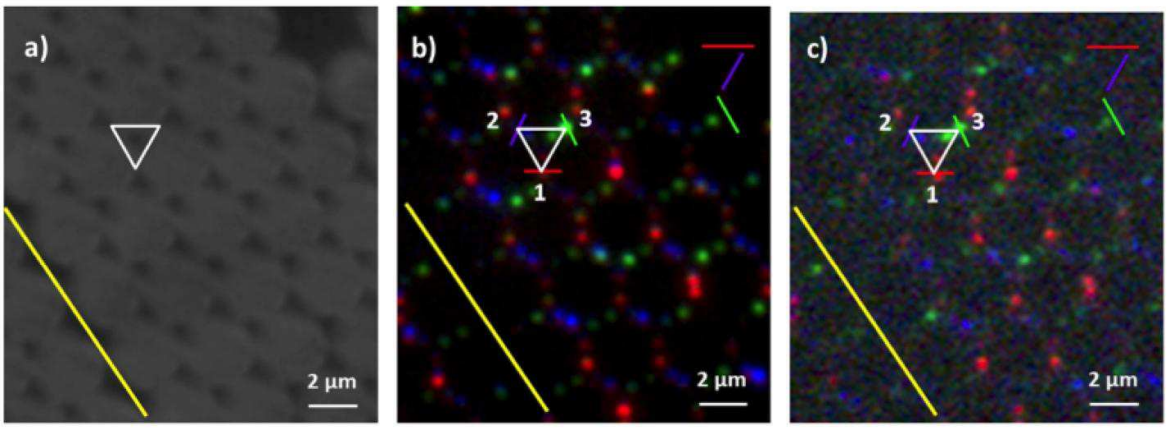

Figure 2: a) Optical image. b) Merged image of three different measured 2PF-images or c) SHG images, respectively, each taken with a different plane of polarisation of the incident light. The incident polarisation plane of the blue, red and green images are depicted by a line on the image in these respective colours. As a guide to the eye, the white triangle corresponds in each of the three images. In b) and c) the tips of the drawn triangle are decorated with the direction of the plane of polarisation that corresponds to the highest 2PF or SHG-intensity for that tip. Note that schematic presentation of the structure, the drawn white triangles are displayed larger than actual, in order that all light generated by triangles be presented with the drawings. The yellow line is a guide to the eye to show a defect in the Au-triangle array. Along this defect, no 2PF and SHG is detected.

this noise level the detected SHG and 2PF intensity of the triangle tips is on average 10 and 65 times higher. As we can not detect the SHG and 2PF generated by the bulk of the faulty structures, and as the SHG and 2PF generated by the tips is spread out over a spot the size of the diffraction limit, the numbers are an underestimation of the effective enhancement factor. Since the higher order and dipole mode are very well separated in our structure (over 1000 nm in wavelength), the recorded images are direct observations of the nonlinear enhancement caused by the higher order mode.

Figure 2 also shows that both SHG and 2PF are most effectively generated when the plane of polarisation of the incident light is oriented perpendicularly to the direction of the tip. This 'puzzling' polarisation dependance of the nonlinear response was noted before, in the context of femtosecond laser patterning using nanostripes and larger sized metallic

triangles [22],[24]. However, in the case of the nanostripes studied by Valev *et al.* [24] the detected polarisation dependance is explained by the fact that the laser induces melting of the structure on the local scale, causing elongation of the nanostripes (formation of a resonant cavity). Thus, depending on the wavelength of light and the length of the cavity, different plasmon resonance modes could be excited. However, this finding was not specially emphasised in the article [24] since the authors' primary objective was to explain the origin of the light induced nanopatterns (nanobumps). Additionally, Kolloch *et al.* [22] describes nanopatterning of gold triangles and the effect of a particular resonance (dipolar and higher order mode) on nanopattern formation. In the case when the wavelength of the laser matches with a higher order mode plasmonic resonance, Kolloch *et al.* observed the same unusual polarisation dependence, quite different from polarisation dependance caused by dipole mode enhancement [13]. Since nanopatterning did not occur in our study, it is likely that the observed polarisation dependance of the nonlinear response is caused by the effect of the higher order mode.

Here we also note that we tried to study smaller metallic triangles, with 135 nm edge length (made from spheres with radius 630 nm [13]), that exhibit a nice matching between the fundamental wavelength and the dipolar response. However, the nonlinear optical intensity decreased during the measurement, indicating that the sample changed under irradiation (melted or patterned). This observed nanopatterning made it impossible for us to perform a full nonlinear optical study using dipolar modes of metallic triangles.

To clarify these results the near-field optical properties of the same triangular array have also been numerically studied. Figure 3 shows the calculated electric field profile (more specifically the module of the enhanced field, which is the total field divided by the incident field) for a vertically incident plane wave at a wavelength of 800 nm, with two perpendicular incidence polarisations (white arrows in Figure 3a and 3b, respectively). These profiles can be attributed to the excitation of a higher order mode. Indeed, it is clearly visible that the largest fields are generated on the triangular tips that are aligned perpendicular to the polarisation direction. The fundamental dipole-like resonance has maxima at opposite ends of the triangles (which 'samples' or feels the complete triangle), but for these (relatively large) particles this resonance happens at much larger wavelengths simulations show the fundamental resonance at 2.55 μm, see SI for the dipolar field profile at this wavelength in function of the incident polarisation. At smaller wavelengths, such as 800 nm as in Figure

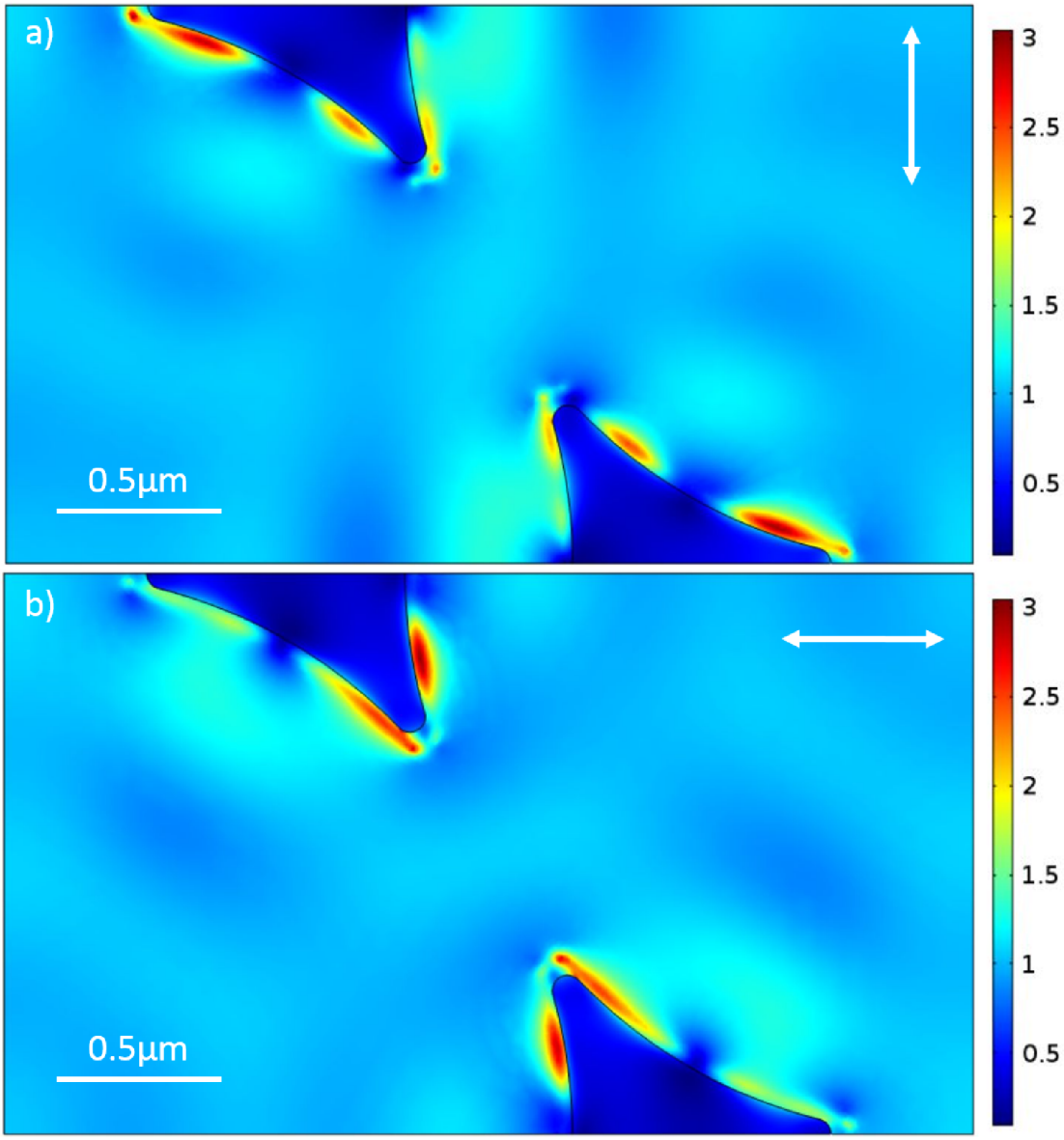

Figure 3: Simulated electric field enhancement profile in a plane 20 nm above the substrate. (a) For vertically incident polarisation and (b) for horizontally incident polarisation. The white arrows indicate the respective polarisation of the incident wave. The light has a wavelength of 800 nm and is perpendicularly incident on the substrate.

3, the particle will resonate over a smaller typical length scale (only a part of the triangle), which is possible by sampling sections in-between the extremities of the triangle, so that the hot-spots are not at the 'typical' tips.

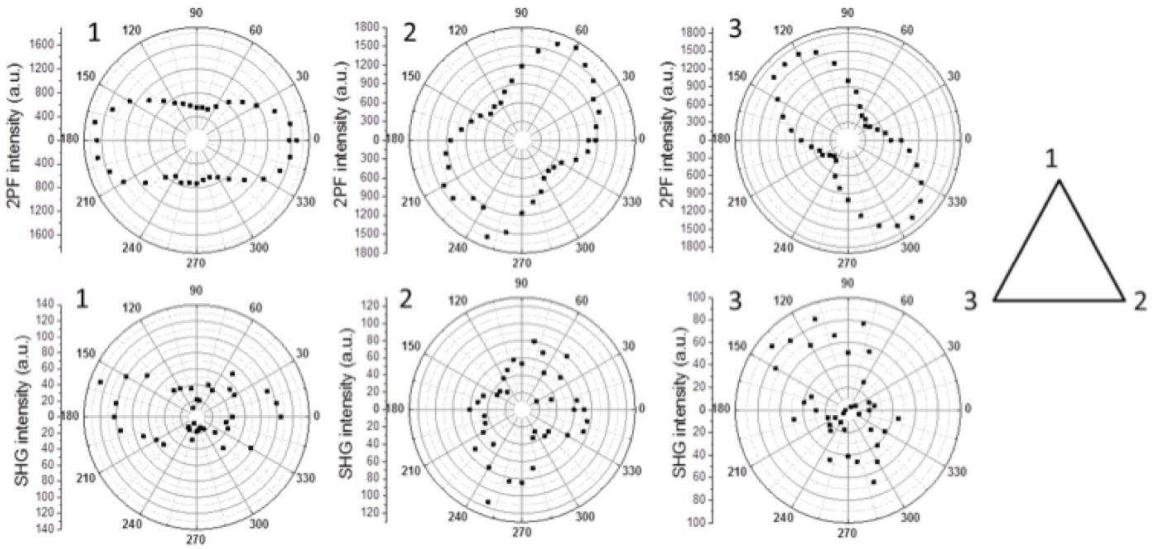

Figure 4: (top row) Measured 2PF intensity and (bottom row) SHG intensity in function of the polarisation angle of the incident light. The numbers assign for which tip of the metallic triangle the 2PF or SHG intensity is shown, see the sketch on the right.

The results in Figures 2 and 3 show that the nonlinear response is determined by the strength and distribution of the near-field caused by the excitation of a higher-order localized surface plasmon mode. The calculated profiles match the experimentally observed hot-spots and polarisation dependance.

In addition, Figure 4 shows the 2PF and SHG intensity in function of the plane of polarisation of the incident light, for each triangle tip. Indeed, in all cases, the strongest 2PF and SHG response is found when the plane of polarisation is oriented perpendicularly to the tip direction.

For the SHG polar plots the signal-to-noise ratio is limited. In the supporting information we added SHG-images and corresponding polar plots, that were taken with the SHG-microscope with a lower spatial resolution to gain a higher signal-to-noise ratio. In the supporting figures the polar plots show more clearly that the SHG-intensity is strongest when the plane of polarisation of the incident light is oriented perpendicularly to the direction of the tip.

The 2PF and SHG intensity as a function of incident polarisation (Figure 4) corresponds nicely with the calculated electric field profiles for different polarisations. The SHG and 2PF

responses follow the spatial distribution of the optical near-fields, induced by the size, shape and orientation of the triangles within an array. For example, the horizontal polarisation (Figure 3a and 3b) shows stronger localisation of the electric field on the tips of the triangle side perpendicular to the polarisation, similar to the SHG and 2PF responses (Figure 4, data corresponding to tip 1). Similarly, for vertical polarisation (Figure 3b) the field is stronger for the tip opposite the side parallel to the polarisation, similar to the SHG and 2PF responses (Figure 4, data corresponding to tip 2 and 3). The differences in near-field distribution within triangles for different polarisations of the incident light result in different intensity of SHG signal and 2PF as a function of polarisation. These results show that the near-field strength and profile of the higher order plasmon resonance fully determines the SHG and 2PF responses of the gold triangles. The presented results additionally confirm the previously published observation about the effect of the higher order mode on femtosecond patterning [22],[24].

Furthermore, we investigate to which extent the generated SHG- and 2PF-light is polarised. In Figure 5 we show 2PF-images (with lower spatial resolution as compared to Figure 2 to obtain a higher signal-to-noise ratio) without analyzer (a-c), with an analyzer that transmits horizontally polarised light (d-f) or vertically polarised light (g-i), respectively. In Figure 6 we show the corresponding SHG-images. During image capture, the camera recorded for each pixel the intensity on that pixel added with the intensity on the four neighbouring pixels. This leads to a lower spatial resolution, but a significantly higher signal-to-noise ratio

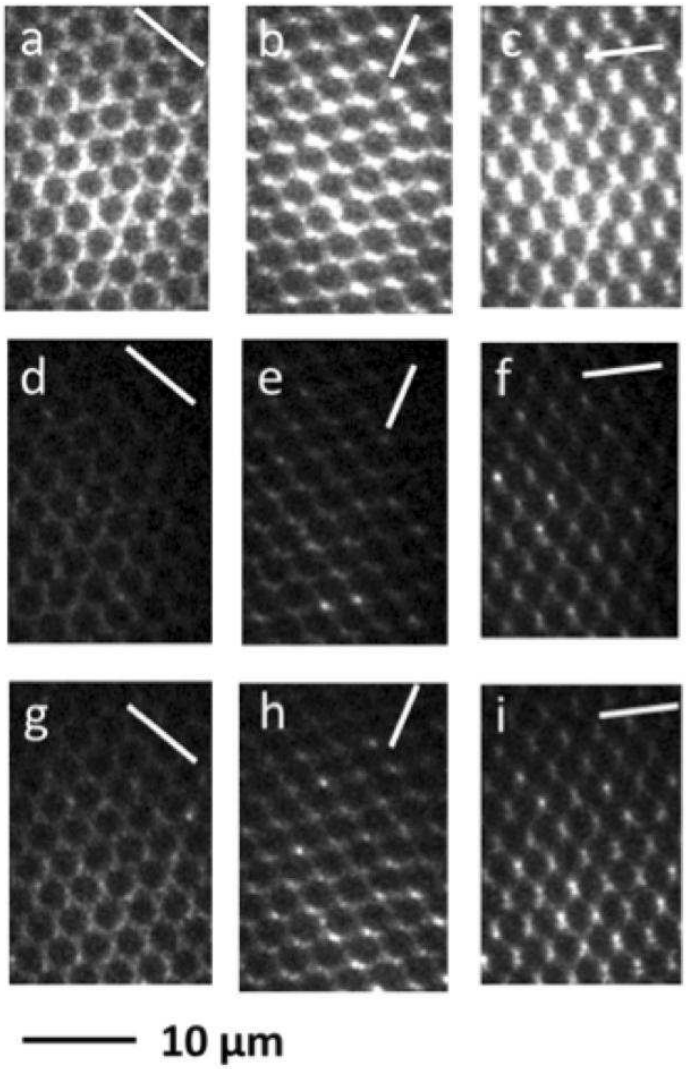

Figure 5: Measured 2PF-images of the Au-triangles. The plane of polarisation of the incident light is depicted by the white bar on each image. Images (a-c) are taken without analyzer, while (d-f) and (g-i) are taken with an analyzer that transmits horizontally and vertically polarised light, respectively.

.

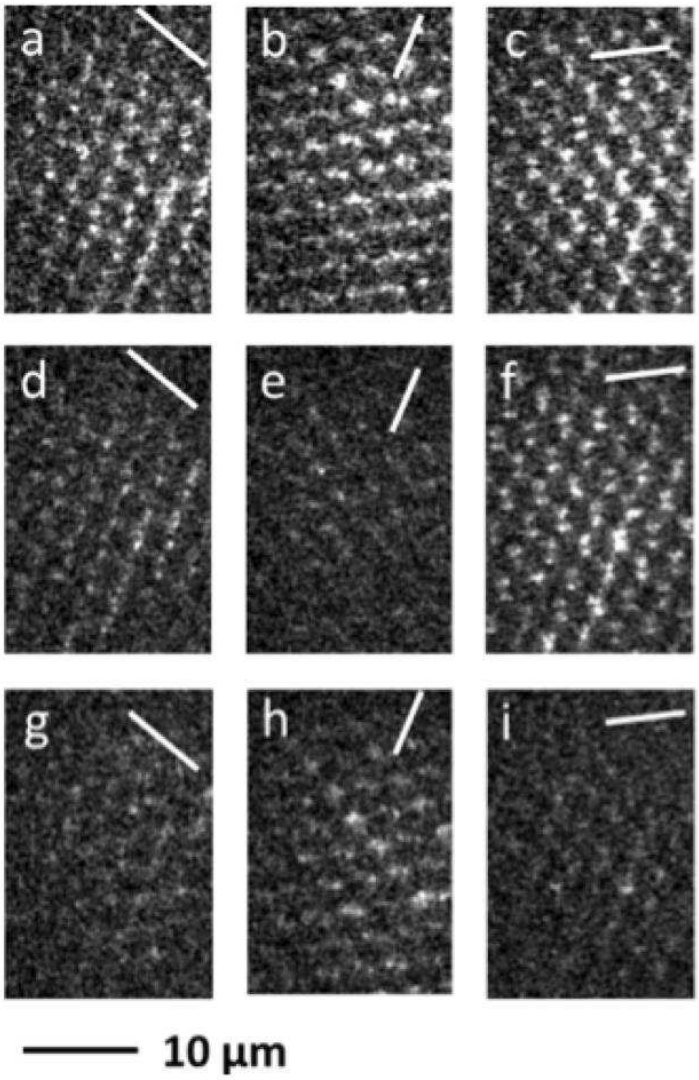

Figure 6: Measured SHG-images of the Au-triangles. The plane of polarisation of the incident light is depicted by the white bar on each image. Images (a-c) are taken without analyzer, while (d-f) and (g-i) are taken with an analyzer that transmits horizontally and vertically polarised light, respectively.

.

For SHG, when the plane of polarisation of the incident light is close to parallel with the plane of polarisation of the detected SHG-light (the case in Figure 6f and h), a significant amount of SHG is detected. In contrast, when the plane of polarisation of the incident light is close to perpendicular to the plane of polarisation of the detected light (Figure 6e and i), hardly any SHG-light is detected. This means that the generated SHG-light is strongly polarised, and the plane of polarisation of the generated light corresponds to the plane of polarisation that generates the SHG-light.

When we make the same comparison for the 2PF-images (comparing Figure 5e with 5h, and Figure 5f with 5i), the 2PF-intensity is hardly affected by the orientation of the analyzer. This shows that the generated 2PF is largely unpolarised. These results are understandable, as SHG is essentially a coherent process, leading typically to polarised SHG-light, while 2PF is a non-coherent process that commonly creates unpolarised light.

III. CONCLUSION

In conclusion, we experimentally prove that the higher order mode of the plasmonic arrays can be used to enhance the nonlinear optical response. Additionally, we observe an atypical polarisation dependence of the SHG caused by a higher order plasmonic resonance that matches well with simulated near-field profiles. Furthermore, we confirm that the communication between the triangles is negligible due the large distance between their tips, so that the recorded optical response is localised within hot-spots at triangle tips. In the end, this study shows that the simplicity of the nanosphere lithography technique and the strength of the higher order resonance could be used for many applications in which the enhancement of nonlinear optical processes as well as control of the polarisation direction is needed.

IV. METHODS

Transmission spectroscopy

The transmission spectroscopy was measured using a Perkin-Elmer Lambda 900 UV–vis–NIR spectrophotometer.

Scanning electron microscope

Scaning electron microscope (SEM) images were recorded on a field-emission scanning electron microscope (FESEM, EOL JSM-6700F).

Nonlinear optical microscope

The light source is a Ti-Sapphire laser (Spectra-Physics, Tsunami, 100 fs pulses with a repetition rate of 80 MHz). The wavelength of 800 nm is chosen. A Glan-Taylor polarizer is placed in the beam path, after which a zero-order half-wave plate for 800 nm (Thorlabs) is placed. By rotation of the half-wave plate, the plane of polarisation of the laser light incident on the sample can be changed. A longpass red filter (Schott, RG665, 1 mm) blocks transmittance of second-harmonic light generated by the optics earlier in the beam path and inside the laser. A lens (f = 7.5 cm) is positioned such that the spotsize plane has a diameter of 500 μm. The following parts are part of an inverted microscope (Olympus, IX71): the objective, a filter carousel and a tube to which the camera is connected. As objective a 100x oil-immersion objective was used. The filter set for the second-harmonic light consists of a bandpass filter (Schott, BG39, 2 mm) and an interference filter (Melles-Griot, F10-400, centre wavelength 400 nm, FWHM 10 nm). The filter set for the two-photon fluorescence transmits light from 420 – 650 nm. If applicable, a Glan-Taylor analyzer was placed in front of the filter set. The transmitted light is detected by an EM-CCD camera (Hamamatsu, C9100-13). Data were collected and analyzed with the HoKaWo software package provided with the camera

Simulations

The simulations are performed with COMSOL Multiphysics 4.4, a commercial finite element based software package. The symmetry of the lattice and the studied polarisation allow us to reduce the computation on one cell using proper boundary conditions as depicted in Figure 3. The gold triangles are shaped via a 3000 nm diameter sphere. The three sides of the basis triangle are 900 nm long. The vertical 40 nm thickness is grown along the sphere, this curvature leads to the top triangle being slightly smaller than the basis triangle (see SI for a detailed depiction). The mesh grid is maximum 10 nm wide in the gold, 130 nm in the air and 90 nm in the glass substrate. The latter is optically described by a refractive index of 1.5 and gold parameters are taken from Palik [29].

Acknowledgments

All authors warmly acknowledge R. Morarescu (UMONS, UGent) for providing samples for preliminary investigations. B.K. acknowledges financial support from SmartFilm Grant 830039 (ECV12020020892F) in the framework of the Convergence Project and from FRS-FNRS. Furthermore, B.K. fully acknowledges fruitful discussions with prof. P. Damman (UMONS). G.R. and B.M. acknowledge financial support from the Belgian Science Policy Office under the project "Photonics@be" (P7-35) and from the Fonds National de Recherche Scientifique (FNRS) in Belgium. T.V. and M.K.V. acknowledge the financial support of the KU Leuven (GOA and PDM).BK, BM and TV acknowledge support from the COST MP1403 project.

[1] Z. Jacob, MRS Bulletin, 2012, **37**, 76

[2] M. Kauranen, A. V. Zayats, Nature Photonics, 2012, **6** 737,

[3] D. Lanterbecq, R. V. Deun, R. Morarescua, P. Damman, B. Kolaric, Opt. Comm., 2013, **152**, 308

[4] P. Fauche, S. Ungureanu, B. Kolaric, and R. A. L. Vallee, J. Mat. Chem. C, accepted, DOI: 10.1039/C4TC01787K

[5] A. Abass, S. R. K. Rodriguez, T. Ako, T. Aubert, M. Verschuuren, D. Van Thourhout, J. Beeckman, Z. Hens, J. Gomez Rivas, B. Maes, Nano Lett., 2014, **14**, 5555

[6] S. Ungureanu, B. Kolaric, J. Chen, R. Hillenbrand, R. A. L. Vallée, Nanophotonics, 2013, **2(3)**, 173

[7] F. Tam, G.P. Goodrich, B. R. Johnson, N. J. Halas, Nano Lett., 2007, **7**, 496

[8] N. Halas, et al, Chem. Rev., 2011, **111**, 3913

[9] Seungchul Kim Jonghan Jin Young-Jin Kim, In-Yong Park Yunseok Kim Seung-Woo Kim,Nature,2008, **453**,757

[10] M. Agio, A. Alu, Optical Antennas, Cambridge University Press, 2013

[11] R. Micheletto, H. Fukuda, M. Ohtsu, Langmuir, 1995, **11**,3333

[12] F. Burmeister et al, Langmuir, 1997, **13**,2983

[13] R. Morarescu, H. Shen, R. A. L. Vallee, B. Maes, B. Kolaric, P. Damman, J. Mat Chem.,

2012, **22**, 11537

[14] K. D. Ko, et al Nano Lett., 2011, **11**, 61

[15] S. Viarbitskaya et al, Nature Materials, 2013, **12**, 426

[16] L. E. Hennemann et al, Beilstein J. Nanotechnol, 2012,**3**, 674

[17] T. W. Ebbesen, Nature, 2006, **440**, 5

[18] J. Grandidier, et al, Nano Lett., 2009, **9**, 2935

[19] H. Husu, et al, Nano Lett., 2012, **12**, 673

[20] V. K. Valev, V. K. et al. Nano Lett., 2009, **9**, 3945

[21] V. K. Valev, et al. ACS Nano, 2011, **5**, 91

[22] A. Kolloch, T. Geldhauser, K. Ueno, H. Misawa, J. Boneberg, A. Plech, P. Leiderer, Appl. Phys. A, 2011, **104**, 793

[23] R. Morarescu, L. Englert, B. Kolaric, P. Damman, R. A. L. Vallee, T. Baumert, F. Hubenthal, F. Trager, J. Mater. Chem., 2011, **21**, 4076

[24] V. K. Valev, et al, Opt. Lett., 2013, **38**, 2256

[25] P. Yang, H. Portales, M. P. Pileni, J. Phys. Chem. C, 2009, **113**, 11597

[26] K. L. Shuford, M. A. Ratner, G. C. Schatz, J. Chem. Phys., 2005, **123**, 114713

[27] S. Van Cleuvenbergen, G. Hennrich, P. Willot, G. Koeckelberghs, K. Clays, T. Verbiest, M. van der Veen, J. Phys. Chem. C, 2012, **116**, 12219

[28] M. van der Veen, B. Sels, D. De Vos, T. Verbiest, J. Am. Chem. Soc., 2010, **132**, 6630

[29] E. D. Palik, Handbook of Optical Constants of Solids, Academic Press, New York, 1985